View Article Online / Journal Homepage / Table of Contents for this issue
Dynamic Article Links

Journal of Materials Chemistry

Cite this: J. Mater. Chem., 2012, 22, 13050

www.rsc.org/materials

PAPER

Polymer-dispersed liquid crystal nanocomposites comprising montmorillonite clay modified by conducting pentamerous oligoaniline

Tsung-Yen Tsai,*[ab] Chun-Yi Lee,[a] Chen-Ju Lee,[b] Mu-Yin Lin[a] and Wei Lee*[bcd]

Received 6th March 2012, Accepted 1st May 2012
DOI: 10.1039/c2jm31379k

Published on 04 May 2012. Downloaded by National Chiao Tung University on 28/04/2014 23:12:59.

Pentamerous oligoaniline (POA) was protonated with sulfuric acid to form emeraldine salts (ES) and then intercalated in montmorillonite (MMT) CL120 to develop a functional conductive organo-layered material. The characteristics of the modified clay CL120/ES-POA were analyzed by wide-angle X-ray diffraction (WAXD) to find the *d*-spacing of the MMT layer distance, and by Fourier transform infrared (FTIR) spectroscopy for the oligoaniline functional group in CL120/ES-POA, and high-resolution thermogravimetric analysis (TGA) to determine the theoretical intercalation capacity of the modifying agent in the clay. We successfully intercalated the ES-POA into the MMT by ionic exchange reaction. Polymer-dispersed liquid crystal (PDLC) composites were prepared from the modified clay of 1 wt% loaded in the mixtures of 49 wt% photosensitive monomer and 50 wt% nematic liquid crystal (NLC), in a specific case, so as to generate novel functional nanocomposites. The hybridization of CL120/ES-POA clearly improved the electro-optical properties of the PDLCs. In this work, doping CL120/ES-POA at 1 wt% beneficially lowered the driving voltage by almost 70%, increased the transmission contrast ratio by five times and reduced the response time from 4.6 to 0.7 ms at 25 V_{rms} at the expense of the viewing-angle properties.

1 Introduction

Typical PDLC composites contain submicron-size NLC droplets randomly encapsulated in a continuous polymer matrix.[1] Following polymerization-induced phase separation (PIPS)[2] between transparent conducting substrates, a PDLC film can be switched between an intensely scattering state and a transparent state by applying an electric field. In the absence of external fields, the NLC molecules in a PDLC device are oriented randomly, and the incident light is scattered due to the mismatch of the refractive indices of the NLC droplets (n_{eff}) and the polymer matrix (n_p), rendering the sample opaque or translucent. Under sufficiently strong electric fields, the NLC directors are aligned in the direction of the electric fields within the NLC droplets ($n_{eff} = n_o$), allowing the effective refractive index of the NLC to match that of the polymer ($n_o \approx n_p$).[3–5] Therefore, the PDLC composite appears transparent. The electro-optical characteristics are conducive to a variety of PDLC-based applications, such as switchable windows,[6–8] display devices,[9–13] and optical devices.[14–18]

Recently, materials scientists have begun to investigate to what extent nanoparticles (NPs) can be hybridized with materials, including a metal,[19] a metal oxide,[20–22] a semiconductor,[23] and an inorganic layered material,[24–27] in PDLC films to affect the optoelectronic properties. The research goal of these investigations is primarily to improve the contrast ratio and reduce the driving voltage for optimization in industrial applications. In addition, filling different inorganic materials in PDLC hybrids often improves the physical properties of the polymer composite and modifies the phase-separated morphology.[25,26] Also, the physical properties of NLCs are markedly affected because of the possibility of surface plasmon excitation or anchoring[28] at the NP–polymer interface.[19] This is a noticeably large value in comparison with PDLC composites that are reinforced with common inorganic NPs without the replacement of both the NLC molecules and the polymer materials. However, electronically conducting organic polymers or oligomers, such as aniline,[29,30] thiophene,[31] pyrrole,[32] acetylene,[33] phenylenevinylene,[34] and others,[35,36] have promise for producing unusual composites and electrochromic materials. Of particular note is the predominance of aniline, an environmentally stable and technologically important conducting polymer whose electrical conductivity can be adjusted by oxidation and reduction chemistry.[37]

The present work reports a novel organic/inorganic functional PDLC composite, where montmorillonite (MMT) as a dopant was modified with a conjugated conducting oligoaniline, with the

[a]*Department of Chemistry, Chung Yuan Christian University, Chung-Li 32023, Taiwan. E-mail: yen@cycu.edu.tw; Fax: +886-3-265-3399; Tel: +886-3-265-3342*
[b]*Master Program in Nanotechnology and Center for Nanotechnology, Chung Yuan Christian University, Chung-Li 32023, Taiwan*
[c]*Department of Physics, Chung Yuan Christian University, Chung-Li 32023, Taiwan. E-mail: wlee@cycu.edu.tw; Fax: +886-3-265-3299; Tel: +886-3-265-3228*
[d]*College of Photonics, National Chiao Tung University, Tainan 71150, Taiwan. E-mail: wlee@nctu.edu.tw; Fax: +886-6-303-2535; Tel: +886-6-303-2121ext. 57826*

This journal is © The Royal Society of Chemistry 2012

View Article Online

Published on 04 May 2012. Downloaded by National Chiao Tung University on 28/04/2014 23:12:59.

modified clay characterized by WAXD (PANalytical, PW3040/60 XPert Pro), high-resolution TGA (SII NanoTechnology, TG/DTA 6200) and FTIR (JASCO, FT/IR-460 plus). The influence on the electro-optical properties was studied by examining the contrast ratio, transmittance, switching voltage, and response time of the pristine and various doped PDLC films.

2 Experimental

2.1 Materials and preparation of the modified clay

NTC-C34, an octahedral-substituted sodium-type MMT, with the chemical formula $Na_{0.89}(Al_{3.11}Mg_{0.89})(Si_8)O_{20}(OH)_4 \cdot 1.75H_2O$ and a cation exchange capacity (CEC) value of 168 meq per 100 g was supplied from China Glaze Co., Ltd. In this work, the clay is referred to as CL120. The clay was added to deionized water at room temperature (25 °C) and stirred for 24 h by swelling to extend the MMT gap. The modified POA filler, with the chemical formula *N*-aminophenyl-*N*′-phenyl-*p*-phenylenediamine and a morphology form of emeraldine-bases (EB), was obtained from the Organic–Inorganic Hybrid Material Laboratory in the Department of Chemistry at Chung Yuan Christian University.[38] It was doped with cations to assume an emeraldine-salt (ES) form (Fig. 1) by using a sulfuric acid solution at pH 0.98 and then stirring under the same conditions as mentioned for swelling CL120. The CL120 swelling solution with swollen MMT and the solution containing the ES form of POA were evenly mixed at 15 °C in an ice bath and then stirred for 24 h to execute the ion exchange reaction. After repeated washing in ethanol solution (90 vol%), the modified clay—CL120/ES-POA—was centrifuged and then dried for 12 h by vacuum freeze-drying.

2.2 Fabrication of PDLC nanocomposites

The materials for fabricating conventional PDLC films included a Norland optical adhesive (NOA65) and a NLC (E7) purchased from Aldrich and E. Merck, respectively. The optical adhesive NOA65 produced by Norland is a photo-polymerizable agent sensitive to ultraviolet (UV) radiation. This polymer precursor, consisting of reactive monomer, photoinitiator (benzophenone) and reactive oligomer, is hardened through photopolymerization when cross-linking takes place under UV exposure. The PDLC in this work was made from a mixture of 50 wt% E7 (50 − *x*) wt% NOA65, and a small amount (*x* wt%, *x* = 0, 0.5, 1, 2) of CL120/ES-POA. A novel organic/inorganic functional PDLC nanocomposite was manufactured using the as-prepared conditions explained in our previous report.[27] Generally, one of the constituents was changed while the other components remained fixed, allowing the convenient investigation of the system's electro-optical properties. Our subsequent consideration of PDLC composites took into account the CL120/ES-POA filler at 0.5, 1, and 2 wt %, thus fixing the contents of E7 and NOA65. The hybrid solution was heated to 80 °C and then slowly introduced by capillary action into empty planar cells with a cell gap of around 12.40 ± 0.15 μm. When the prepared samples were cooled to room temperature, they were cured by UV exposure at 11 mW cm^{-2} for 10 min at wavelength λ = 365 nm. A field emission scanning electron microscope (HITACHI S-4100) was used to study the morphology of the polymer matrix and a transmission electron microscope (JEM-2010, JEOL) was used to observe the dispersed morphology of the filler in polymer composites at 200 kV. Note that the NLC droplets were first removed by *n*-hexane for such characterizations.

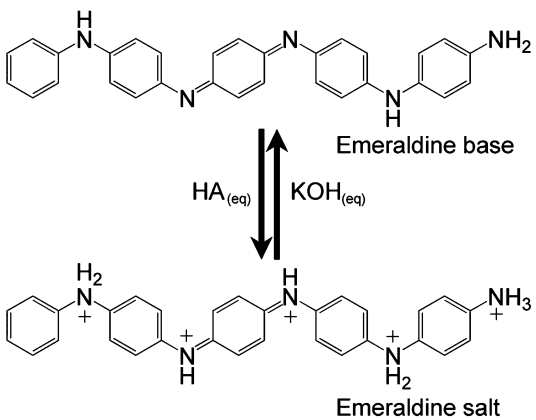

Fig. 1 Chemical structures of the pentamerous oligoaniline protonated from EB-form to ES-form.

2.3 Measurement of electro-optical properties

An optical system was used to characterize the electro-optical properties of our PDLC composites. A normally incident He–Ne laser beam (λ = 632.8 nm) was passed through a polarizer in front of a PDLC sample. The measurement system[27] was controlled by a LabVIEW 8.6 graphical program for automation. An electrical voltage was applied to the composite film using conductive copper tapes, which were adhered under the ITO electrodes on the cell and provided an unobstructed conductive path to an arbitrary function generator. Transmittance–voltage plots were acquired with a variable applied square-wave voltage at 1 kHz. The threshold voltage V_{th} and the driving voltage V_d represent the applied voltages required to obtain 10% and 90% transmittance, T_{10} and T_{90}, in the film, respectively. The two characteristic voltages are related to some material parameters as follows:[39]

$$V_c \approx \frac{1}{c}\frac{d}{R}\sqrt{\frac{K(l^2-1)}{\varepsilon_0 \Delta\varepsilon}} \quad (1)$$

where R is the characteristic drop radius, d is the film thickness, K is a Frank elastic constant for distortion of the nematic texture, l ($\equiv a/b$) is the droplet aspect ratio (with a and b representing the droplet's major radius and minor radius, respectively), ε_0 (= 8.854 × 10^{-12} F m^{-1}) is the permittivity in vacuum, and $\Delta\varepsilon$ is the dielectric anisotropy of the NLC. In the case where the frequency f (= 1 kHz in this study) is greater than σ_p/ε_p and $\sigma_{LC}/\varepsilon_{LC}$, with σ symbolizing the electric conductivity and the subscripts "p" and "LC" denoting the polymer and the LC, respectively, the prefactor c, standing for the field-gathering effect due to the dielectric mismatch or conductivity σ of the droplets and the surrounding matrix, can be approximated as:

$$c = \frac{3\varepsilon_p'}{2\varepsilon_p' + 2\varepsilon_p'} \quad (2)$$

View Article Online

Published on 04 May 2012. Downloaded by National Chiao Tung University on 28/04/2014 23:12:59.

where ε' represents the real part of the dielectric constant. The characteristic voltages can then be rewritten as:

$$V_c \approx \frac{d}{3a}\left[\frac{\varepsilon'_{LC}}{\varepsilon'_p} + 2\right]\sqrt{\frac{K(l^2-1)}{\varepsilon_0 \Delta\varepsilon}} \quad (3)$$

The contrast ratio was deduced by calculating the ratio of the maximum transmittance at high voltage to the minimum transmittance at zero voltage. Rise times defined as the durations from T_{10} rising to T_{90} were measured after turning on voltages at 25, 50, 100, and 150 V_{rms}. The viewing-angle experiment was carried out by observing the incident-angle dependence of the optical transmittance at 200 V_{rms}, which was well beyond V_d. Dielectric spectroscopy using an Agilent E4980A LCR meter with a probe signal at 50 mV_{rms} in the sinusoidal waveform was performed to investigate the frequency-dependent dielectric properties of various hybrid PDLC cells.

3 Results and discussion

3.1 Structural characterization of modified MMT–CL120/ES-POA

The ES-POA was intercalated in the interspace of CL120 MMT by substituting a sodium ion (Na^+) with a quaternary ammonium ion group (NH_3^+). To observe the modifier stretching the *d*-spacing in the MMT interlayer, WAXD was scanned over a Bragg diffraction angle (2θ) range from 2 to 65 degrees for the CL120/ES-POA powder. In a pristine sample, CL120 showed a strong d_{001} diffraction peak at $2\theta = 7.00°$ (*d*-spacing = 1.26 nm). On the other hand, CL120/ES-POA exhibited a typical intercalated structure by increasing the *d*-spacing to 1.52 nm as illustrated in Fig. 2. In the case of the powdered CL120/ES-POA, a shift of the MMT d_{001} diffraction signal to a broader peak at a smaller angle was observed in that the POA molecules tended to align sideways in a layered structure in the clay (the theoretical length of the POA is 2.0–2.4 nm and its width is ~0.5 nm). Note that the neat clay had a higher order of layer stacking to enhance the X-ray diffraction intensity, yielding pronounced higher-order signals. In comparison, the order of the layered agglomerations in the modified clay intercalated with ES-POA was damaged to a certain degree, causing higher-order diffractions to be hardly detected. In addition, the modified clay CL120/ES-POA contained an organic component of the same capacity as the holder. The resulting smaller capacity of the inorganic clay led to the weakening of the characteristic peaks. Detailed investigations by FTIR and TGA, which will be discussed later, proved that the modified POA was intercalated in the MMT layers.

Fig. 3 presents the FTIR spectra of neat CL120, CL120/ES-POA and EB-POA. Infrared spectroscopy is a useful method for detailing the oligomer in the MMT. One observes a general correspondence between CL120/ES-POA and POA for benzene ring C–C stretching modes near 1600 and 1500 cm^{-1}, for the secondary C–N stretching band near 1050 cm^{-1}, for a possible phenyl-nitrogen stretching band near 1300 cm^{-1}, and for an out-of-plane phenyl-hydrogen mode near 800 cm^{-1}. The vibrations near 740 and 690 cm^{-1} are due to the out-of-plane wagging of five adjacent phenyl hydrogens on the end phenyl in the POA oligomer.[38] Moreover, the mineral surface is characterized by a broad and strong absorbance at 1150–900 cm^{-1}, a hydroxide mode (bending of silicon-hydroxide) at 1641 cm^{-1}, a silicon–oxygen–silicon mode at 1039 cm^{-1}, an Al–O mode at 517 cm^{-1}, and a Mg–O mode at 463 cm^{-1} in the CL120 MMT. FTIR measurements testified to the existence of the absorption bands of various functional groups from the POA grafts, while the primitive MMT features are also retained.

TGA thermograms were used to study the weight-loss percentage of the organic POA in CL120, signifying the theoretical intercalation capacity defined as the percentage of weight in the CEC of the organic filler. Fig. 4 depicts the thermal treatment, at a rate of 10 °C min^{-1} from 30 °C to 900 °C in an air environment (flow: 100 ml min^{-1}), on pristine CL120, CL120 incorporating the ES-form of POA, and CL120 impregnated with the EB-form of POA. The weight loss of EB-POA intercalated in CL120 was dictated by physical adsorption without undergoing acidic doping. According to this figure, the intercalation capacity, determined by the weight loss due to organic decomposition in the 200–850 °C region of the thermogram, was about 23.51%. Note that the intercalation capacity of the ES-form of POA was calculated to be about 87.26%. The dopant with the ES-form could significantly enhance the ion exchange rate because amine nitrogen could be protonated and efficiently supplant the dispersed sodium ions in the MMT galleries.

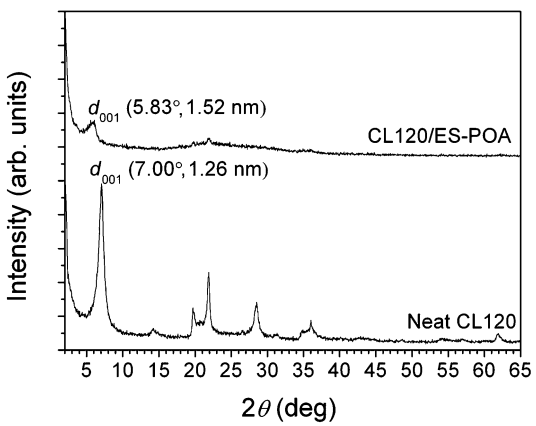

Fig. 2 WAXD patterns of neat clay CL120 and modified clay CL120/ES-POA.

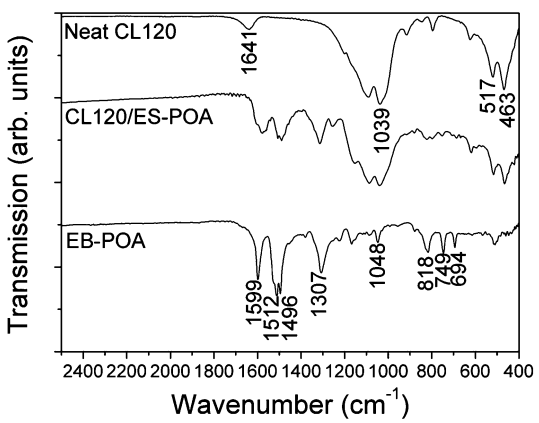

Fig. 3 FTIR spectra of the neat CL120, the modified clay CL120/ES-POA, and the EB-form of POA.

 This journal is © The Royal Society of Chemistry 2012

View Article Online

Published on 04 May 2012. Downloaded by National Chiao Tung University on 28/04/2014 23:12:59.

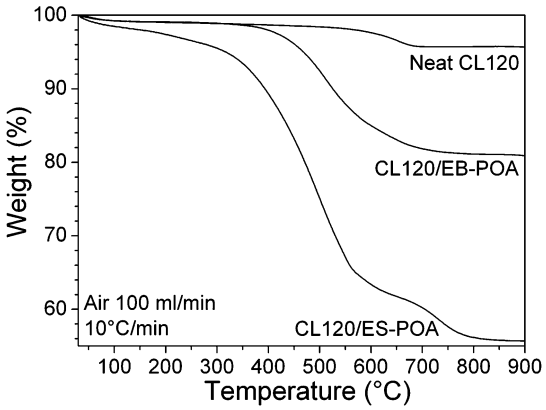

Fig. 4 Temperature dependence of weight.

Evidence for increased intercalation capacity by TGA measurements confirmed that ES-POA was successfully exchanged into MMT.

3.2 Morphologies of droplets and dielectric properties of PDLCs

Fig. 5a–e show the morphologies of five different PDLC samples taken with a field emission scanning electron microscope (FESEM). In accordance with the photographs, the averaged geometrical parameters of the LC droplets in these samples are presented in Table 1. The droplet size R, defined as the arithmetic average of a and b, of 0.55 μm for the undoped PDLC was smaller than that of the PDLC containing 1 wt% CL120/ES-POA (0.93 μm). Note that the LC droplets shown in Fig. 5c were more spherical in the PDLC sample comprising 0.5 wt% CL120/ES-POA. Increasing the amount of the dopant to 1 wt% in the PDLCs resulted in larger droplet sizes with a more irregular morphology (see Fig. 5d). Note that Fig. 5d looks more like a mesoporous network structure rather than a typical PDLC morphology with droplets embedded in a polymeric matrix. We are certain that it was caused by the modified clay filler that dramatically affected the phase separation. It is a pity that a sound explanation cannot be provided at this moment. Fig. 5e shows the morphology of a polymeric composite impregnated with ES-POA. Fig. 5f is a tunneling-emission micrograph of a PDLC film consisting of the CL120/ES-POA filler. It evidently shows the partial intercalation and exfoliation of the modified nanoclay in the polymer.

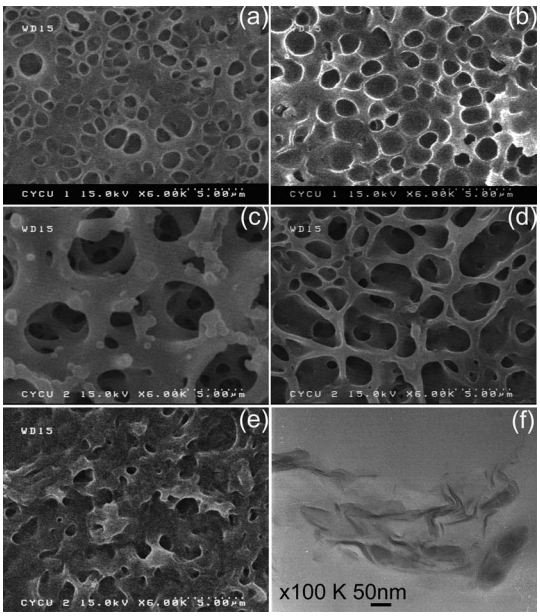

Fig. 5 FESEM micrographs of various PDLC samples comprising (a) no dopant, (b) 3 wt% CL120, (c) 0.5 wt% CL120/ES-POA, (d) 1 wt% CL120/ES-POA, and (e) 1 wt% ES-POA. (f) TEM micrograph of a PDLC sample comprising 1 wt% CL120/ES-POA.

According to eqn (1), the larger the size of the droplets, the lower the characteristic voltages. Plugging the data in Table 1 into eqn (1) permits a lowered V_d, indeed, but by only about 35% rather than the observed 70% drop for the sample with 1 wt% CL120/ES-POA filler. Obviously, an accurate analysis would require data obtained from more sophisticated measurements of the various parameters given by eqn (3).

In order to further understand the dopant effect on the dielectric properties of the PDLCs, we experimentally examined the respective influence of CL120/ES-POA on the dielectric spectra of the NOA65 composites and E7. Various undoped and doped NOA65/E7 and NOA65 cells were exposed to UV light at 365 nm wavelength for 10 min to induce complete cross-linking for polymerization. The dielectric spectra of the thus-formed PDLC– and polymerized NOA65–CL120/ES-POA samples are shown in Fig. 6a and b, respectively.

Fig. 6a reveals the dielectric permittivity ε' as well as the dielectric loss ε'' in the frequency range of 50 Hz–10 kHz at room temperature. In the low-frequency region ($f < 100$ Hz), characterized by the space-charge polarization, ES-POA hybridized in a PDLC exhibited a greater dielectric loss than that of any other PDLC samples; we can thus deduce that the conducting oligomer ES-POA additive by itself acted as an unwanted ionic impurity in the PDLC system. Comparatively, a slight rise in dielectric loss was observed in the PDLC–CL120/ES-POA sample, in that the clay CL120 held on to the conductive oligomer to restrain it from dispersing in the LC domains. Note that loading neat clay in the PDLC film (PDLC–CL120) had minimal influence on the dielectric permittivity of a pristine PDLC,[40] while it decreased the dielectric loss in the low-frequency region because the clay platelets could effectively trap mobile ions in the cell.[41]

At first glance, in the dielectric spectra (Fig. 6a), the dielectric permittivity of the PDLC sample containing 1 wt% CL120/ES-POA was smaller than that of the sample containing 1 wt% ES-POA at 1 kHz. However, we observed that the dielectric permittivity of polymerized NOA65 was promoted to a similar level by doping either ES-POA or CL120/ES-POA as shown in Fig. 6b. This implied that the modification of the dielectric properties of the PDLCs by the dopants might primarily originate from the dopant-containing LC. Indeed, Fig. 7 clearly shows that the dielectric behaviors, particularly for the perpendicular component $\varepsilon_\perp$, of various LC samples resembled those of the corresponding PDLC samples. It is also clear from Fig. 7a that both fillers, ES-POA and CL120/ES-POA, enhanced the dielectric anisotropy ($\Delta\varepsilon = \varepsilon_\parallel' - \varepsilon_\perp'$) in E7 at 1 kHz. Although the LC sample consisting of ES-POA possessed a slightly larger dielectric anisotropy, the trade-off of the use of the conducting

View Article Online

Published on 04 May 2012. Downloaded by National Chiao Tung University on 28/04/2014 23:12:59.

Table 1 LC droplet sizes and geometries in various PDLC films deduced from FESEM data. (σ's are the standard deviations and N denotes the number of droplets counted for the calculations)

Dopant in PDLC	a (μm)	σ_a (μm)	b (μm)	σ_b (μm)	R (μm)	σ_R (μm)	l	N
None	0.57	0.32	0.54	0.29	0.55	0.31	1.06	100
CL120, 3 wt%	0.77	0.44	0.74	0.35	0.75	0.40	1.03	58
CL120/ES-POA, 1 wt%	1.03	1.49	0.83	0.93	0.93	1.25	1.25	53
CL120/ES-POA, 0.5 wt%	1.11	1.32	1.06	1.42	1.08	1.37	1.05	23
ES-POA, 1 wt%	0.54	0.77	0.52	0.64	0.53	0.72	1.04	33

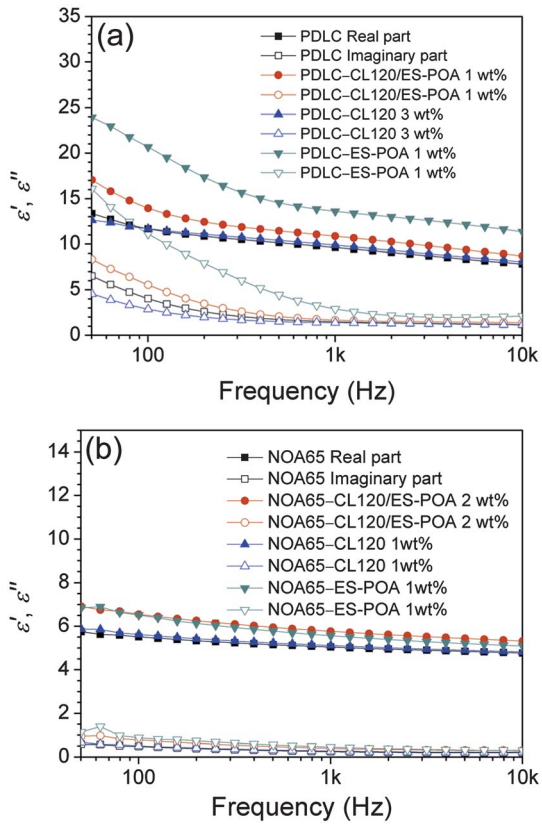

Fig. 6 Real (solid symbols) and imaginary (hollow symbols) parts of the frequency-dependent dielectric functions of (a) various PDLC films and (b) different dopants in polymerized NOA65 at room temperature.

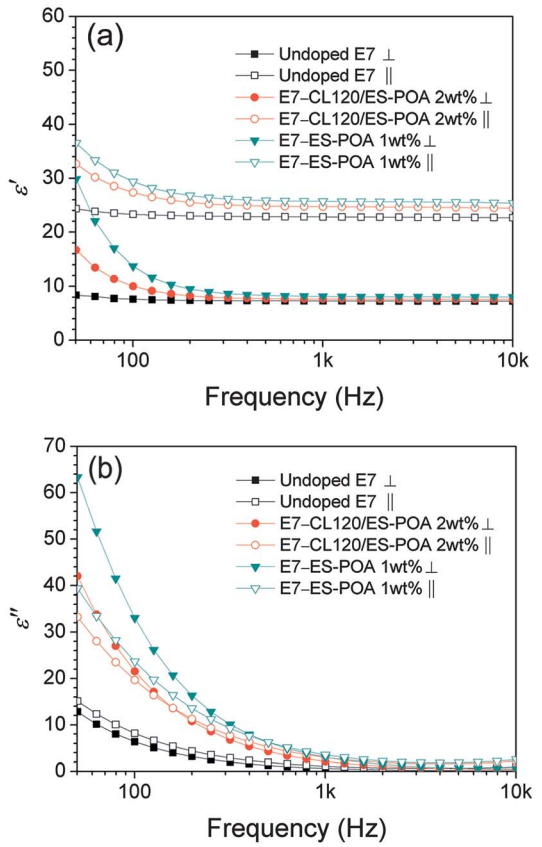

Fig. 7 Perpendicular (solid symbols) and parallel (hollow symbols) components of (a) the real and (b) imaginary parts of the frequency-dependent dielectric functions of undoped and doped E7 at room temperature.

oligomer compared with the functionally modified clay was an enhanced but undesired field-screening effect due to excessive mobile charge in the cell, as revealed by Fig. 7b. In contrast, for the counterpart composed of CL120/ES-POA, we believe that ES-POA was trapped in the interlayer region of the clay, thereby demoting the concentration of mobile ions while promoting the dielectric anisotropy and, in turn, leading to a lower operating voltage for the PDLC cells containing CL120/ES-POA.

3.3 Electro-optical properties of PDLCs

The electro-optical properties of PDLCs are related to the size and structure morphology of the LC droplets.[39] We fixed all the experimental parameters except the dopant material and dopant concentration in the mixture. For the viscous colloidal solution of the mixture of E7 and NOA65 containing a loading of 2 wt% CL120/ES-POA, we observed that the colloidal introduction into empty cells was hardly achieved because the organically modified dopant created a strong interaction, dominated by hydrogen bonding as well as π–π stacking, between CL120/ES-POA and the molecules of the host (including NOA65 and E7) and increased the viscosity of the system. For this reason, we ruled out consideration of PDLC samples doped with organically modified clay beyond 1 wt%.

Fig. 8 shows the transmittance–voltage curves of various PDLC composites, revealing a V_{th} of 9.43, 7.53, 6.81 and 3.88 V_{rms} for an undoped PDLC, a PDLC doped with 3 wt% CL120, a PDLC doped with 1 wt% CL120/ES-POA and a PDLC doped with ES-POA at 1 wt%, respectively. Our experimental results show that the clay-doped samples had noticeably lower V_{th} and V_d values, as displayed in Table 2,

 This journal is © The Royal Society of Chemistry 2012

View Article Online

Published on 04 May 2012. Downloaded by National Chiao Tung University on 28/04/2014 23:12:59.

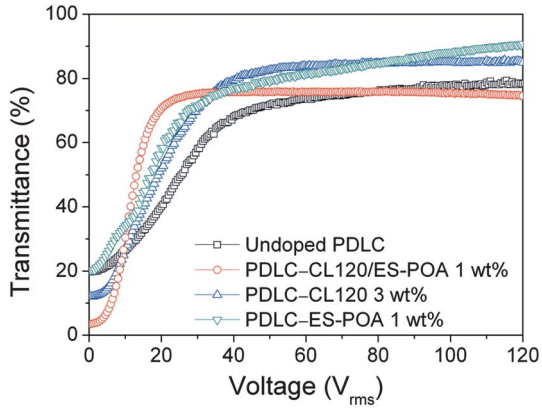

Fig. 8 Voltage dependence of the transmittance curves for undoped and doped PDLCs.

where the data were deduced from the voltage-dependent curves of transmittance. Notably, V_d for the neat PDLC was dramatically decreased from 64.93 V_{rms} to 19.29 V_{rms} by hybridizing 1 wt% CL120/ES-POA. This is a drastic reduction by 70%. Both Fig. 8 and Table 2 imply that the electric field was more effectively transmitted to the NLC droplets in the PDLC system impregnated with 1 wt% modified clay than in the counterpart containing 3 wt% pristine CL120. Fig. 8 also shows that POA in the ES-form dispersed in a PDLC composite could not efficiently reduce the characteristic voltages. It is clear that the desired dopant effect in terms of a reduction in the operation voltage can be achieved by dispersing nanoclay (CL120 in this study) into PDLC films and the best result comes from the doping of the modified clay CL120/ES-POA. The periodically layered structure of clay (Fig. 2) serving as a carrier can promote the dispersion of ES-POA in the PDLC structure because ES-POA is intercalated in the CL120 galleries in the PDLC film (see Fig. 2 and 3). The inclusion of protonated conjugate oligomers in the PDLC system enhances the electric conductivity, thereby reducing V_{th} and V_d.

As shown in Fig. 9a, the rise times at 25 V_{rms} were 4.6, 3.0, and 0.7 ms for the neat PDLC and PDLCs doped with 3 wt% CL120 and 1 wt% CL120/ES-POA, respectively. This result demonstrates that the rise time was remarkably reduced by 85% by adding 1 wt% CL120/ES-POA. When the applied voltage across a PDLC cell was increased, the rise time declined and eventually reached a saturation level near 0.03 ms at 200 V_{rms}. Obviously, CL120/ES-POA dispersed in a PDLC is undoubtedly an interesting nanocomposite that is promising for applications based on the above-mentioned electro-optical properties.

Table 2 Threshold (V_{th}) and driving (V_d) voltages and contrast ratio (CR) of various PDLC samples deduced from voltage–transmittance curves

Dopant in PDLC	V_{th} (V_{rms})	V_d (V_{rms})	CR
None	9.43	64.93	4.30
CL120, 3 wt%	7.53	39.18	7.16
CL120/ES-POA, 1 wt%	6.81	19.29	21.40
CL120/ES-POA, 0.5 wt%	5.33	22.89	11.00
ES-POA, 1 wt%	3.88	91.04	2.72

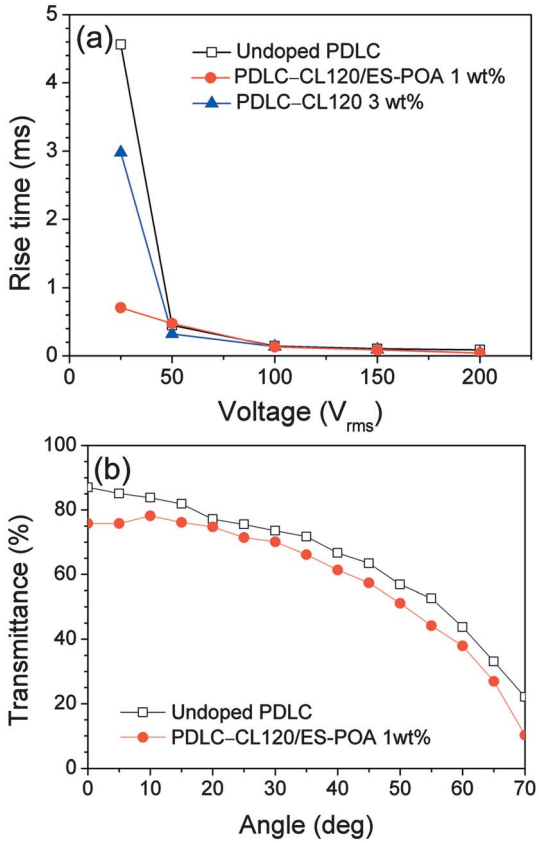

Fig. 9 (a) Rise times of three PDLC samples at various voltages and (b) transmittance of the undoped and doped PDLCs as a function of the incident angle at 200 V_{rms}.

PDLCs are known to suffer from off-axis haze, yielding lower transmittance at larger angles of incidence. In order to further examine the potential of the clay-doped composites for practical applications, we studied the angle dependence of transmittance of the PDLC–CL120/ES-POA. Fig. 9b depicts the transmittance curves of two PDLC nanocomposites with and without a dopant at viewing angles ranging between 0° and 70°. One can see that the transmittance was lowered by 12.91% to 53.50% from 0° to 70° by adding the dopant into the PDLC structure. Although the undoped counterpart outperformed the doped one in the entire angle range investigated, the transmittance of the doped one still warranted its photonic application within 60°. We speculated that light propagation would be hampered by the layered structure of clay or by some irregular structures of the LC droplets which induced light scattering.

4 Conclusion

In summary, the layered structure in clay was successfully interchanged with POA molecules on an orderly sideways basis by ion-exchange reaction. A transition of POA from the EB-form to the ES-form was achieved by employing a strong acidic medium. ES-POA was then mixed with the MMT clay CL120 to become an interesting organic–inorganic hybrid material. It is recognized that loading relatively low concentrations of CL120/ES-POA produced dramatic improvements in the electro-optical

View Article Online

Published on 04 May 2012. Downloaded by National Chiao Tung University on 28/04/2014 23:12:59.

properties of PDLCs. The hybridization of CL120/ES-POA at 1 wt% lowered the driving voltage by almost 70%, promoted the contrast ratio by 5 times, rapidly polarized the NLC directors at 25 V_{rms}, and approached a viewing angle in a manner depending on the applied field. Beyond these results, this work stresses the key role of inorganic layered materials and functional organic molecules, such as conducting oligomers, in designing novel nanocomposites to conspicuously improve the electro-optical properties for PDLC applications in photonics.

Acknowledgements

The authors are indebted to J.-M. Yeh for providing the POA conducting oligomers and to China Glaze Co., Ltd. for providing sodium MMT. We also thank Chung Yuan Christian University, the National Science Council and the Ministry of Economic Affairs of Taiwan, R.O.C. for financial support under grants, NSC 95-2113-M-033-008-MY3, NSC 98-2622-M-033-003-CC2 and 99-EC-17-A-08-S1-143.

References

1 H. S. Kitzerow, *Liq. Cryst.*, 1994, **16**, 1–31.
2 B. Yan, J. He, Y. Fang, X. Du, Q. Zhang, S. Wang, C. Pan and Y. Wang, *Eur. Polym. J.*, 2009, **45**, 1936–1940.
3 G. Spruce and R. D. Pringle, *Electronics & Communications Engineering Journal*, 1992, **4**, 91–100.
4 D. A. Higgins, *Adv. Mater.*, 2000, **12**, 251–264.
5 Y. J. Jeon, Y. Bingzhu, J. T. Rhee, D. L. Cheung and M. Jamil, *Macromol. Theory Simul.*, 2007, **16**, 643–659.
6 P. S. Drzaic, *J. Appl. Phys.*, 1986, **60**, 2142–2148.
7 C. D. Sheraw, L. Zhou, J. R. Huang, D. J. Gundlach, T. N. Jackson, M. G. Kane, I. G. Hill, M. S. Hammond, J. Campi, B. K. Greening, J. Francl and J. West, *Appl. Phys. Lett.*, 2002, **80**, 1088–1090.
8 P.-C. Wang and A. G. MacDiarmid, *Displays*, 2007, **28**, 101–104.
9 H. Ono and N. Kawatsuki, *Polym. Bull.*, 1995, **35**, 365–370.
10 F. Roussel, R. Chan-Yu-King and J. M. Buisine, *Eur. Phys. J. E: Soft Matter Biol. Phys.*, 2003, **22**, 293–300.
11 C. Hoppe, M. Galante, P. Oyanguren and R. Williams, *Mater. Sci. Eng., C*, 2004, **24**, 591–594.
12 D. Cupelli, F. P. Nicoletta, S. Manfredi, G. D. Filpo and G. Chidichimo, *Sol. Energy Mater. Sol. Cells*, 2009, **93**, 329–333.
13 S. Park and J. W. Hong, *Thin Solid Films*, 2009, **517**, 3183–3186.
14 H. Ren, Y.-H. Lin, Y.-H. Fan and S.-T. Wu, *Appl. Phys. Lett.*, 2005, **86**, 141110.
15 S.-K. Fan, C.-P. Chiu and J.-W. Lin, *Appl. Phys. Lett.*, 2009, **94**, 164109.
16 H.-T. Dai, X.-W. Sun, D. Luo and Y.-J. Liu, *Opt. Express*, 2009, **17**, 19365–19370.
17 P. C. Lallana, C. Vazquez, B. Vinouze, K. Heggarty and D. S. Montero, *Mol. Cryst. Liq. Cryst.*, 2009, **502**, 130–142.
18 D. Cupelli, F. P. Nicolett, S. Manfredi, M. Vivacqua, P. Formoso, G. D. Filpo and G. Chidichimo, *Sol. Energy Mater. Sol. Cells*, 2009, **93**, 2008–2012.
19 A. Hinojosa and S. C. Sharma, *Appl. Phys. Lett.*, 2010, **97**, 081114.
20 A. Kovalchuk, L. Dolgov, L. Bugayova and O. Yaroshchuk, *Mol. Cryst. Liq. Cryst. Sci.*, 2005, **427**, 191/[503]–200/[512].
21 O. Yaroshchuk, L. Dolgov and A. Kiselev, *Phys. Rev. E: Stat., Nonlinear, Soft Matter Phys.*, 2005, **72**, 051715.
22 W. Li, M. Zhu, X. Ding, B. Li, W. Huang, H. Cao, Z. Yang and H. Yang, *J. Appl. Polym. Sci.*, 2009, **111**, 1449–1453.
23 S. C. Sharma, *Mater. Sci. Eng., B*, 2010, **168**, 5–15.
24 T.-Y. Tsai, S.-W. Lu, Y.-P. Huang and F.-S. Li, *J. Phys. Chem. Solids*, 2006, **67**, 938–943.
25 Y.-P. Huang, Y.-M. Chang, T.-Y. Tsai and W. Lee, *Mol. Cryst. Liq. Cryst.*, 2009, **512**, 167/[2013]–178/[2024].
26 Y.-M. Chang, T.-Y. Tsai, Y.-P. Huang, W.-S. Cheng and W. Lee, *J. Opt. A: Pure Appl. Opt.*, 2009, **11**, 024018.
27 T.-Y. Tsai, C.-Y. Lee, C.-J. Lee, W. C. Chang, W. Lee and P.-C. Chen, *J. Phys. Chem. Solids*, 2010, **71**, 595–599.
28 B. Jerome, *Rep. Prog. Phys.*, 1991, **54**, 391–451.
29 F. Wudl, R. O. Angus, F. L. Lu, P. M. Allemand, D. Vachon, M. Nowak, Z. X. Liu, H. Schaffer and A. J. Heeger, *J. Am. Chem. Soc.*, 1987, **109**, 3677–3684.
30 L. Chen, Y. Yu, H. Mao, X. Lu, W. Zhang and Y. Wei, *Mater. Lett.*, 2005, **59**, 2446–2450.
31 C. Edder and J. M. Frechet, *Org. Lett.*, 2003, **5**, 1879–1882.
32 R. A. Simon, A. J. Ricco and M. S. Wrighton, *J. Am. Chem. Soc.*, 1982, **104**, 2031–2034.
33 M. Moroni, J. L. Moigne and S. Luzzati, *Macromolecules*, 1994, **27**, 562–571.
34 K. D. Gourley, C. P. Lillya, J. R. Reynolds and J. C. W. Chien, *Macromolecules*, 1984, **17**, 1025–1033.
35 M. Boussoualem, R. C. Y. King, J. Brun, B. Duponchel, M. Ismaili and F. Roussel, *J. Appl. Phys.*, 2010, **108**, 113526.
36 A. Tercjak, E. Serrano, M. Larraaga and I. Mondragon, *J. Appl. Polym. Sci.*, 2008, **108**, 1116–1125.
37 W.-I. Hung, C.-B. Hung, Y.-H. Chang, J.-K. Dai, Y. Li, H. He, S.-W. Chen, T.-C. Huang, Y. Wei, X.-R. Jia and J.-M. Yeh, *J. Mater. Chem.*, 2011, **21**, 4581–4587.
38 S. G. L. W. Shacklette, J. F. Wolf and R. H. Baughman, *J. Chem. Phys.*, 1988, **88**, 3955–3961.
39 K. Amundson, *Phys. Rev. E: Stat. Phys., Plasmas, Fluids, Relat. Interdiscip. Top.*, 1996, **53**, 2412–2422.
40 H.-H. Liu and W. Lee, *Appl. Phys. Lett.*, 2010, **97**, 023510.
41 Y.-P. Huang, H.-Y. Chen, W. Lee, T.-Y. Tsai and W.-K. Chin, *Nanotechnology*, 2005, **16**, 590–594.

 This journal is © The Royal Society of Chemistry 2012